TÜBİTAK

Turkish Journal of Physics

http://journals.tubitak.gov.tr/physics/

Research Article

Turk J Phys
(2013) 37: 289 – 295
© TÜBİTAK
doi:10.3906/fiz-1208-6

Synthesis and optical characterization of $Zn_{1-x}Mg_xS{:}Eu$ nanoparticles

Alexander Nwabueze AMAH,* Audu ONOJA, Richard AKPAGHER
Department of Physics, University of Agriculture, Makurdi, Nigeria

Received: 13.08.2012 • **Accepted:** 18.12.2012 • **Published Online:** 13.09.2013 • **Printed:** 07.10.2013

Abstract: $Zn_{1-x}Mg_xS : Eu^{3+}$ nanoparticles were synthesized by a facile co-precipitation technique with varying magnesium concentrations $(0 \leq x \leq 0.20)$. X-ray diffraction results showed a mixture of cubic and hexagonal structures. There was an observed peak shift towards higher angles, decrease in peak intensities, disappearance of other peaks, and increase in diffraction peak broadening as Mg concentration increased. The estimated average particle sizes ranged from 2.0 nm to 8.79 nm. Scanning electron microscopy results showed smooth and uniform surface morphology. Energy dispersive X-ray studies indicated that the samples contained mainly Zn, S, and Eu because of the low detection limit for Mg. UV-Vis absorption spectrophotometer results showed a blue shift in energy due to quantum confinement as Mg concentration increased.

Key words: $Zn_{1-x}Mg_xS{:}Eu^{3+}$ nanoparticles, quantum confinement, hexagonal structure, particle size

1. Introduction

Semiconductor nanostructured materials in recent times have attracted much research interest due to their remarkable size, shape, surface dependency, and optical, physical, and chemical properties. These unique properties exhibited by semiconductor nanocrystallites as compared to the bulk phase [1] originate from their large surface-to-volume ratio and quantum confinement effect [2].

An important subset of these semiconductor nanocrystals are those doped with a small percentage of dopant to alter their electronic, magnetic, and optical properties for various desired applications [3]. The impurity incorporated transfers the dominant recombination route from the surface state to the impurity state, which improved radiative efficiency and induced emission significantly [4]. The impurity also increases the lattice constant of the host, thus weakening the crystal field and the variation of phonon coupling caused by the doping ion that results in emission at short wavelengths [5].

One important II-VI semiconductor crystal host for doping active ions is ZnMgS. ZnMgS has attracted much attention because of its direct wide band gap energy (3.67 eV) at room temperature, which could be controlled by changing synthesis conditions in order to achieve a desired ultraviolet (UV) and visible spectra range [6]. The crystalline properties of ZnMgS alloy generally may display 3 different structures, the zinc blend (cubic β-ZnS), wurtzite (hexagonal α-ZnS), and rock salt (γ-MgS) [7]. This alloy has large excitonic emission energy, which makes it a strong candidate for applications in UV detection, plasma display, electroluminescent phosphor display, light-emitting diodes, solar cells, laser diode, cladding layers [8], and fabrication of optoelectronic devices in the whole visible range because the band gap can be controlled as a function of Mg concentration, offering a tuning of optical properties [9].

*Correspondence: odunzalex@yahoo.com

Rare earth elements are excellent candidates for luminescence centers of doped nanostructures due to their optical advantages such as sharp fluorescence emission, large stoke shift, no photo-bleaching, and long luminescent time [10,11]. The emission of Eu^{3+} ions varies from blue to red depending on the host lattice due to crystal field effects [10].

In this paper, $Zn_{1-x}Mg_xS$ nanoparticles are doped with Eu^{3+} using a facile co-precipitated chemical method.

2. Experimental procedures

2.1. Materials

The study used zinc sulfate heptahydrate ($ZnSO_4{\cdot}7H_2O$, Kermer Company), magnesium sulfate ($MgSO_4{\cdot}7H_2O$, Sigma Chemical Company), sodium sulfide ($Na_2S \cdot xH_2O$, BDH Chemical Company), europium(III) chloride (Sigma Chemical Company), and ethanol (C_2H_2O, Sigma-Aldrich), and deionized water was used as a solvent. All the reagents were of analytical purity and were used without further purification.

2.2. Preparation of $Zn_{1-x}Mg_xS:Eu^{3+}$ nanoparticles

In a typical procedure, 0.1 M $ZnSO_4{\cdot}7H_2O$ was mixed with an x-molar concentration of $MgSO_4{\cdot}7H_2O$, where x = 0.00, 0.05, 0.10, 0.15, and 0.20, respectively, and a fixed concentration of 5 mol% $EuCl_3 \cdot 6H_2O$ under vigorous stirring to obtain a clear solution. The mixture was then refluxed at 90 °C for 1 h and the heat was turned off to allow the solution to cool at room temperature. Next, 0.35 M $NaS_2 : 2H_2O$ solution was introduced into the above mixture dropwise under continuous stirring. The white precipitate obtained was separated from the solution by centrifugation at 3500 rpm. The precipitate was washed 3 times with deionized water and then 3 times with ethanol to remove dissolved impurities. The precipitate was dried in an oven at 80 °C for 24 h. Finally, the obtained white solid was crushed into fine powder.

2.3. Characterization

X-ray diffraction (XRD) patterns of the samples were obtained using CuKα ($\lambda = 1.5406$ AA) radiation (Radicon MD-10) with a diffraction angle between 13° and 75°. Scanning electron microscopy (SEM) studies were performed using a Carl-Zeiss MA-10 model. UV-Vis absorption spectra were recorded on a Helios AOEL-PD-303 UV spectrophotometer.

3. Results and discussion

3.1. XRD analysis

Figures 1 shows the XRD pattern for $Zn_{1-x}Mg_xS{:}Eu^{3+}$ powder at various Mg concentrations of x = 0.00, 0.05, 0.10, 0.15, and 0.20. The $ZnS:Eu$ at a 0.00 Mg concentration shows the hexagonal structure of zinc sulfide with high intensities. The resolved diffraction peaks are (100), (111), (101), (200), (103), (201), and (202) reflections of mixed cubic and hexagonal structures of ZnS and ZnMgS, respectively (JCPDS No. 891397 and 05-0566). The intensity of the XRD peaks decreases as Mg composition increases.

This agrees with earlier observations [12]. At the higher concentration of x = 0.20, the peak corresponding to the (111) reflection is essentially broadened. This broadening of the peak could arise due to microstraining of the crystal structure as the Mg^{2+} ions substitute the Zn^{2+} ion in the lattice.

The average crystallite sizes were calculated using the Debye–Scherrer formula [5].

$$D = \frac{0.9\lambda}{\beta \cos\theta} \tag{1}$$

Here, λ is the wavelength, D is the average diameter of the crystal, θ is the Bragg angle, and β is the full width at half maximum. The crystallite sizes estimated from the major peaks center at 2θ ranges from 2.00 nm to 8.79 nm.

3.2. Scanning electron microscopy (SEM) analysis

The morphology of the synthesized $Zn_{1-x}Mg_xS{:}Eu^{3+}$ is shown in Figures 2a–2e for x = 0.00, 0.05, 0.10, 0.15, and 0.20, respectively. The surfaces of the samples show microstructure homogeneity. The particles are nearly spherical in nature, showing agglomeration of the particles. The elemental composition studied using energy dispersive X-ray (EDX) (shown in Figure 3 and the Table for x = 0.00, 0.05, 0.10, 0.15, and 0.20) confirms pure $ZnMg:Eu$ with Zn, S, and Eu being well resolved in the spectrum. Mg could not be detected by EDX.

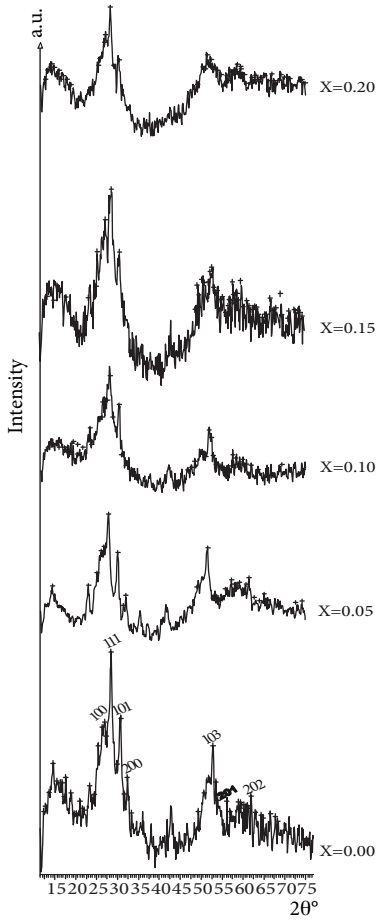

Figure 1. The x-ray powder diffraction pattern of $Zn_{1-x}Mg_xS{:}Eu^{3+}$ nanoparticles ($0 \leq x \leq 0.20$).

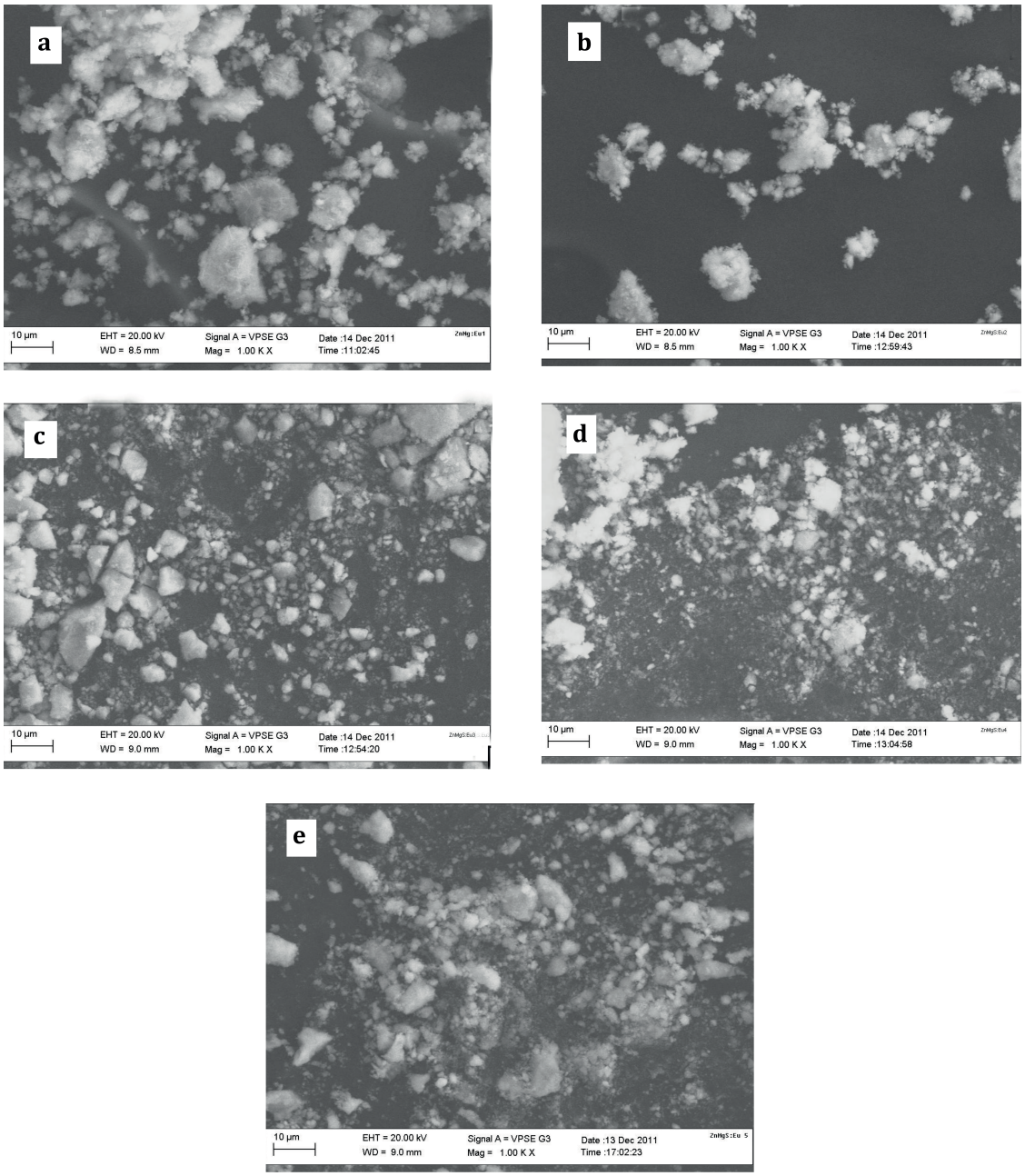

Figure 2. SEM micrographs of Eu^{3+} doped $Zn_{1-x}Mg_xS$: (a) x = 0.0, (b) x = 0.05, (c) x = 0.10, (d) x = 0.15, and (e) x = 0.20.

3.3. UV-Vis absorption spectroscopy

The optical spectra for as-synthesized $Zn_{1-x}Mg_xS{:}Eu^{3+}$ nanoparticles are shown in Figure 4a. The optical absorption spectra have absorption band edges located around 330 nm, 320 nm, 310 nm, 300 nm, and 290 nm for Mg concentrations of x = 0.00, 0.05, 0.10, 0.15, and 0.20, respectively. The respective energy band gap associated with these band edge absorptions was determined from Tauc's relation [13].

Table. EDX results of elemental composition by weights (in grams).

Element	Weight %	Atomic %
CK	46.92	66.65
OK	22.71	24.22
AlK	0.53	0.34
SK	6.57	3.50
CuK	0.47	0.13
ZnK	17.49	4.57
EuL	5.30	0.60
Total	100	

(a) MgZnS:Eu1 for x = 0.00

Element	Weight %	Atomic %
CK	60.29	75.70
OK	19.75	18.65
AlK	1.19	0.67
SK	3.74	1.76
ZnK	13.03	3.01
EuL	2.10	0.21
Total	100	

(b) MgZnS:Eu2 for x = 0.05

Element	Weight %	Atomic %
CK	62.98	77.50
OK	19.30	17.83
AlK	0.81	0.44
SK	3.15	1.45
CuK	0.25	0.06
ZnK	10.94	2.47
EuL	2.57	0.25
Total	100	

(c) MgZnS:Eu3 for x = 0.10

Element	Weight %	Atomic %
CK	56.06	73.88
OK	18.74	18.54
AlK	2.26	1.33
SK	4.96	2.45
ZnK	14.01	3.39
EuL	3.96	0.41
Total	100	

(d) MgZnS:Eu4 for x =0.15

Element	Weight %	Atomic %
CK	61.35	76.68
OK	19.54	18.33
AlK	0.65	0.36
SK	3.76	1.76
ZnK	10.82	2.48
EuL	3.88	0.38
Total	100	

(e) MgZnS:Eu5 for x = 0.20

$$\alpha = \frac{(h\upsilon - E_g)^m}{h\upsilon} \tag{2}$$

Here, α is the absorption coefficient, h is Planck's constant, υ is the frequency, $m = \frac{1}{2}$ for direct band gap, $m = 2$ for indirect band gap, and $m = \frac{3}{2}$ for direct forbidden transitions. The value of the optical band gap was obtained by extrapolating the straight line portion of $(\alpha h\upsilon)^2$ vs. the $h\upsilon$ graph to $(\alpha h\upsilon)^2 = 0$ in Figure 4b. The band gaps obtained are 3.92 eV, 3.95 eV, 3.97 eV, 4.00 eV, and 3.92 eV for Mg concentrations of x = 0.00, 0.05, 0.10, 0.15, and 0.20, respectively. The obtained band gaps are blue-shifted to higher energy relative to the bulk band gap energy of 3.67 eV for ZnS. The blue shift could be caused by the quantum confinement effect.

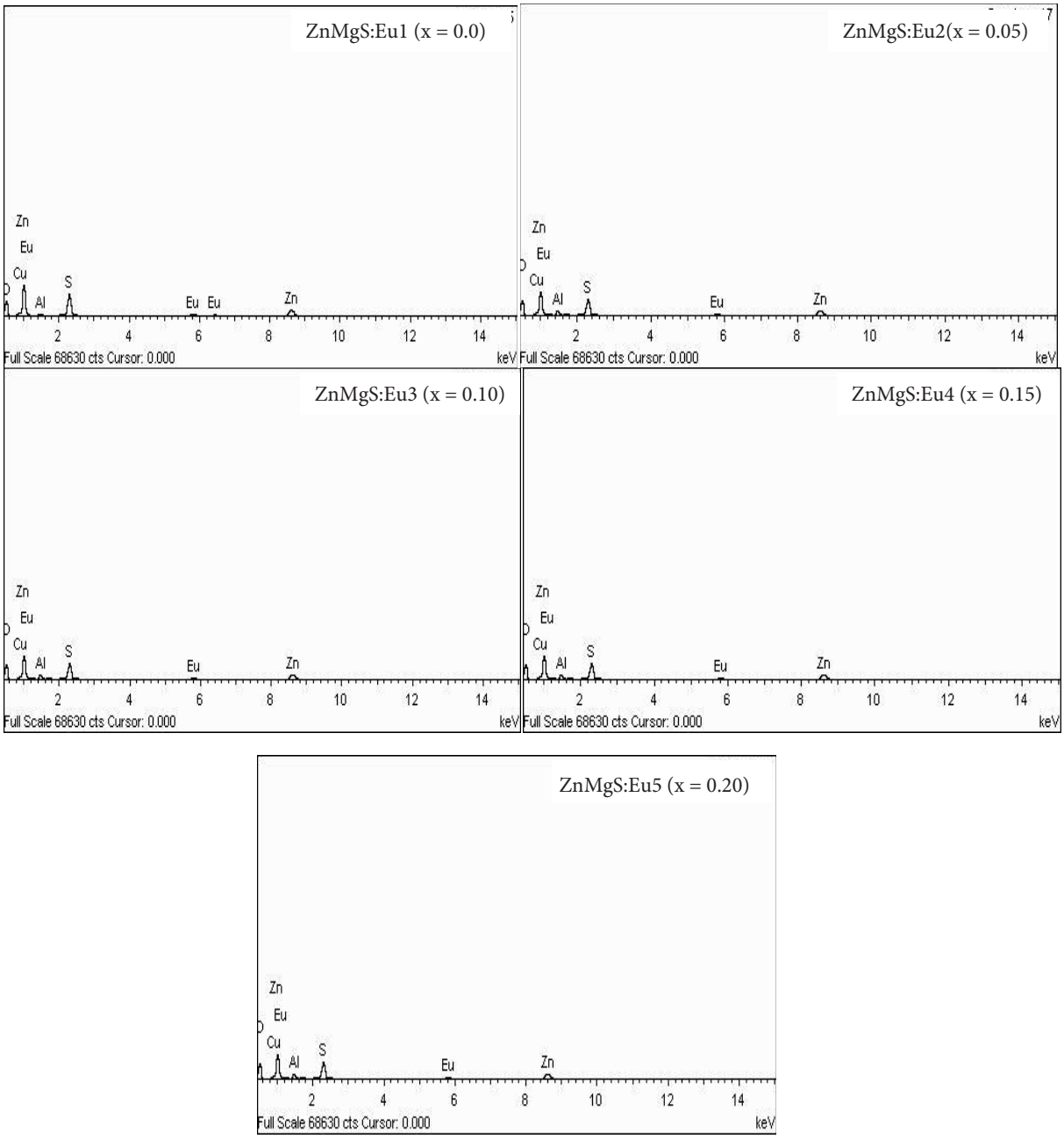

Figure 3. EDX results for Eu^{3+} doped $Zn_{1-x}Mg_xS$ for $0 \leq x \leq 0.20$.

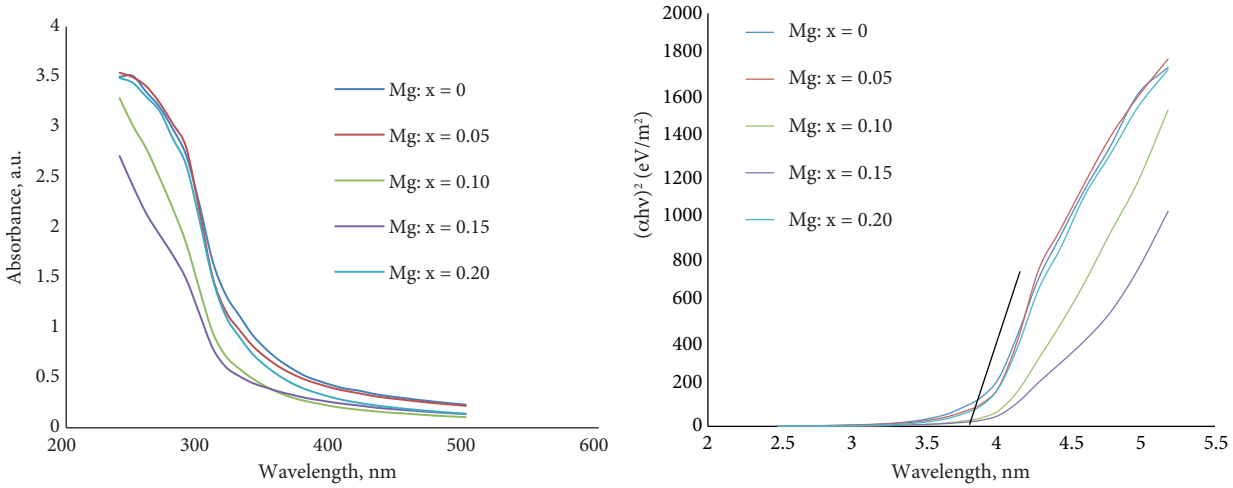

Figure 4. a) UV-Vis absorption spectra of prepared $Zn_{1-x}Mg_xS{:}Eu^{3+}$ nanoparticles; b) The band edges of $Zn_{1-x}Mg_xS{:}Eu^{3+}$ nanoparticles at x = 0.00, 0.05, 0.10, 0.15, and 0.20.

4. Conclusion

$ZnMgS:Eu$ nanoparticles have been synthesized using a precipitation method. This is evident from EDX analysis. The energy band gap of the synthesized nanoparticles shows a blue shift due to quantum confinement effects. The XRD analysis showed a mixed structure of cubic and hexagonal ZnS structure. All the diffraction peaks showed considerable decrease in their intensities with increasing Mg concentration.

References

[1] G. Murugadoss, B. Rajamannan and V. Raimasamy, *J. Nanomater. Bios.*, **5**, (2010), 339.

[2] C. Corrado, Y. Jiang, F. Oba, M. Kozina, F. Bridges and J. Z. Zhang, *J. Phys. Chem.*, **113**, (2008), 3830.

[3] G. H. Li, F. H. Su, B. S. Ma, K. Ding, S. J. Xu and N. Chen, *Phys. Stat. Sol.*, **241**, (2004), 3248.

[4] H. Chander, *Future Luminescent Materials* (Luminescent Materials and Devices Group, Electronic Materials Division, New Delhi, India. 2006) p. 11.

[5] J. Zhang, F. Su, W. Chen, R. Sammynaiken, S. L. Westcott, D. E. McCready, G. Liand and A. G. Joly, *J. Nanosci. Nanotechnol.*, **5**, (2005), 1465.

[6] E. Omurzak, W. Shimokawa, K. Taniguchi, L. Chen, M. Okamoto, H. Iwasaki, M. Yamasaki, Y. Kawamura, S. Sulaimankulova and T. Mashimo, *Jpn. J. Appl. Phys.*, **50**, (2011), 1.

[7] T. Tawara, I. Suemune and S. Tanaka, *J. Cryst. Growth*, **214–215**, (2000), 1019.

[8] L. W. Lu, I. K. Sou and W. K. Ge, *J. Cryst. Growth*, **225**, (2004), 28.

[9] M. Sohe, M. Munoz and M. C. Tamargo, *App. Phys. Lett.*, **85**, (2004), 2794.

[10] V. Singh, J. Zhu, M. K. Bhide and V. Natarijan, *Optical Material*, **30**, (2007), 446.

[11] Y. Du, Y. Zhang, L. Sun and C. Yan, *J. Phys. Chem.*, **112**, (2008), 12234.

[12] M. K. Jayaraj, A. Antony and P. Denesshan, *Thin Films*, **389**, (2001), 284.

[13] A. Slav, *Dig. J. Nanomater. Bios.*, **6**, (2011), 915.